Development of Red-B, a Peroxynitrite Probe for robust fluorimetric analysis under varying physiological pH and oxygen levels

Josefina Pereyra [1,2]; Carolina Prolo[1,2]; Rafael Radi[1,2,3]; Natalia Rios[1,2,3]

[1]Departamento de Bioquímica, Facultad de Medicina, Universidad de la República, Montevideo, Uruguay.
[2]Centro de Investigaciones Biomédicas (CEINBIO), Facultad de Medicina, Universidad de la República, Montevideo, Uruguay.
[3]Programa en Alimentos y Salud Humana (PAyS), Facultad de Medicina, Universidad de la República

josefinapereyra@fmed.edu.uy

Introduction

Oxygen (O_2) contributes in part to the cytotoxic response in macrophages. Over the past decade, several probes have been developed for the selective detection of different oxidants in biological systems. Peroxynitrite ($ONOO^-$), the product of the reaction between nitric oxide ($^{\bullet}NO$) and superoxide ($O_2^{\bullet-}$), is a strong oxidant that can cause biological damage through oxidation and nitration. Typically used boron-based probes for peroxynitrite detection are prone to oxygen-dependent quenching by pO_2 variations and are highly pH sensitive. Therefore, we are developing a group of fluorescent boronate-based probes (Red-BI and its structural analogues Red-BII and Red-BIII, bearing an extended π-conjugated system) derived from xanthene (**Scheme 1**). These probes will complement and expand the use of conventional boronates, enabling accurate cellular detection of peroxynitrite and offering new insights into the role of oxygen in oxidant production within the cellular microenvironment.

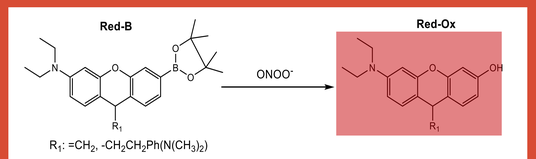

Scheme 1. Generic reaction between Red-B and peroxynitrite

Acknowledgements

References

- Prolo, C., Rios, N., et al. (2018). Fluorescence and chemiluminescence approaches for peroxynitrite detection. FRBM, 128, 59–68.
- Rios, N., et al. Sensitive detection and estimation of cell-derived peroxynitrite fluxes using fluorescein-boronate., 101, 284–295.
- Poronik, Y. et al. (2007). Substituted xanthylocyanines. III. Dyes containing non-symmetrically substituted xanthylium core. Dyes and Pigments, 72(2), 199–207.
- Chevalier, A. et al. (2014). Straightforward Access to Water-Soluble Unsymmetrical Sulfoxanthene Dyes: Application to the Preparation of Far-Red Fluorescent Dyes with Large Stokes' Shifts. Chem.A Europ. Journal, 20(27), 8330–8337.
- Dickinson, B . et al.(2010). A Palette of Fluorescent Probes with Varying Emission Colors for Imaging Hydrogen Peroxide Signaling in Living Cells. JACS, 132, 5906–5915.

Aims

Aim:
Development of a novel group of fluorescent boronate-based probes (Red-B) for peroxynitrite detection, considering changes in the cellular microenvironment.

Specific Objectives:

- To synthesize three fluorescent boronate-based probes derived from xanthene for peroxynitrite detection (Red-BI and its structural analogues Red-BII and Red-BIII).
- To characterize the spectroscopic properties and stability of the fluorophores under varying pH and pO_2 conditions.
- To characterize the reaction kinetics between the probes and different oxidants.

Results

Red-B synthetic route

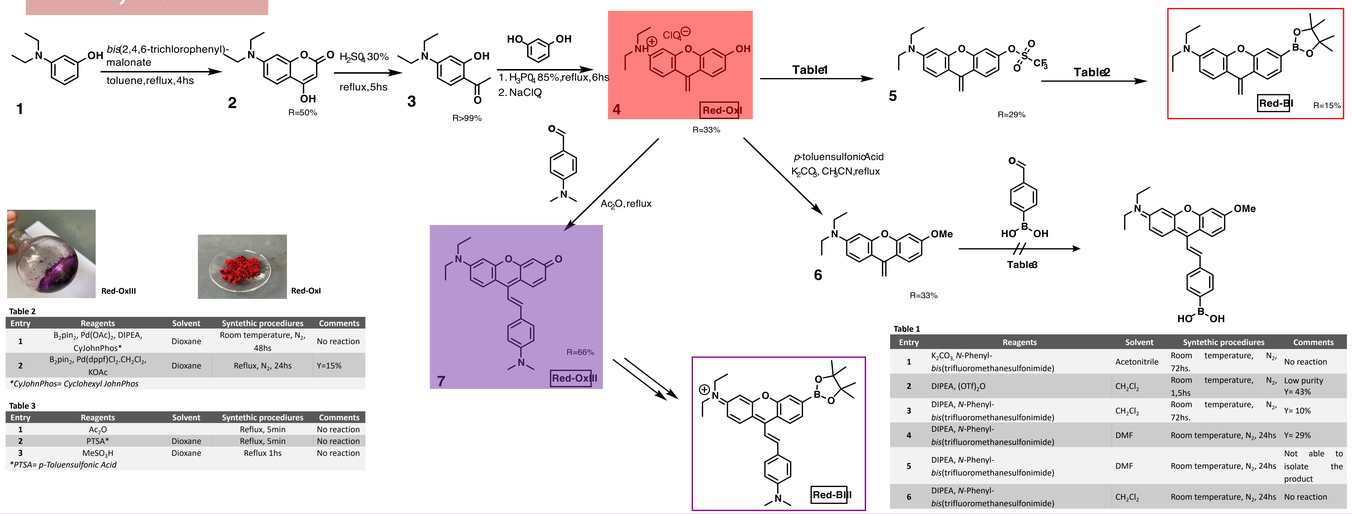

Table 2

Entry	Reagents	Solvent	Syntethic procediures	Comments
1	B_2pin_2, $Pd(OAc)_2$, DIPEA, CyJohnPhos*	Dioxane	Room temperature, N_2, 48hs	No reaction
2	B_2pin_2, $Pd(dppf)Cl_2.CH_2Cl_2$, KOAc	Dioxane	Reflux, N_2, 24hs	Y=15%

CyJohnPhos= Cyclohexyl JohnPhos

Table 3

Entry	Reagents	Solvent	Syntethic procediures	Comments
1	Ac_2O		Reflux, 5min	No reaction
2	PTSA*	Dioxane	Reflux, 5min	No reaction
3	$MeSO_3H$	Dioxane	Reflux 1hs	No reaction

PTSA= p-Toluensulfonic Acid

Table 1

Entry	Reagents	Solvent	Syntethic procediures	Comments
1	K_2CO_3, *N*-Phenyl-*bis*(trifluoromethanesulfonimide)	Acetonitrile	Room temperature, N_2, 72hs.	No reaction
2	DIPEA, $(OTf)_2O$	CH_2Cl_2	Room temperature, N_2, 1,5hs	Low purity Y= 43%
3	DIPEA, *N*-Phenyl-*bis*(trifluoromethanesulfonimide)	CH_2Cl_2	Room temperature, N_2, 72hs.	Y= 10%
4	DIPEA, *N*-Phenyl-*bis*(trifluoromethanesulfonimide)	DMF	Room temperature, N_2, 24hs	Y= 29%
5	DIPEA, *N*-Phenyl-*bis*(trifluoromethanesulfonimide)	DMF	Room temperature, N_2, 24hs	Not able to isolate the product
6	DIPEA, *N*-Phenyl-*bis*(trifluoromethanesulfonimide)	CH_2Cl_2	Room temperature, N_2, 24hs	No reaction

Figure 1: Red-B synthetic route. The synthesis of Red-OxI involves three steps. Red-BI was obtained by the reaction between Red-OxI and a triflation agent (**Table 1**), followed by borylation (**Table 2**). For the obtention of Red-BII, Red-OxI was first methylated and then different reaction conditions were explored as detailed in **Table 3**. Red-OxIII was also synthesized from Red-OxI and *p*-dimethylaminobenzaldehyde. Its subsequent borylation will lead to Red-BIII. All the products were characterized by Nuclear Magnetic Resonance (^1H y ^{13}C-NMR including two-dimensional analyses (COSY, HSQC, HMBC), and tandem Mass Spectrometry (ESI-MS/MS).

Characterization of Red-OxI and Red-OxIII

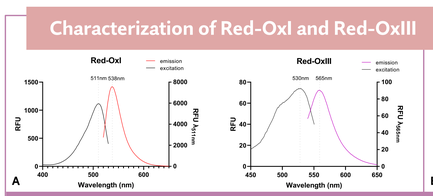

	Red-OxI	Red-OxIII	FI
λ_{exc}(nm)	515	530	490
λ_{em}(nm)	538	565	520
λ_{max} (nm)	515	530	490
ε ($M^{-1}.cm^{-1}$)	67000	7133	76900
Φ_F	0.092	0.045	0.93
τ_F (ns)	0.29 (44.25%) 4.19 (38.13%) 1.30 (17.63%)	*nd*	4.16
pKa	5.68	4.88	2.08 4.31 6.43

nd: not determinated

Figure 2: Spectroscopic characterization of the fluorophores Red-OxI and Red-OxIII. A) Excitation and emission spectrum of Red-OxI (10μM) and Red-OxIII (15μM) at 25°C in sodium phosphate buffer 10mM pH= 7.4. **B)** Summary of spectroscopic properties.

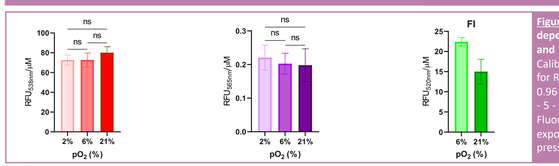

Figure 3 Evaluation of oxygen-dependent quenching of Red-OxI and Red-OxIII fluorescence. Calibration curve slope (URF/μM) for Red OxI (0 - 0.33 - 0.46 - 0.73 - 0.96 - 1.23 - 2.72μM), Red-OxIII (0 - 5 - 10 - 15 - 20 - 25 - 30μM) and Fluorescein (FI) (0 – 0.2 – 0.5μM) exposed to different oxygen pressures (pO_2 =2, 6, 21%).

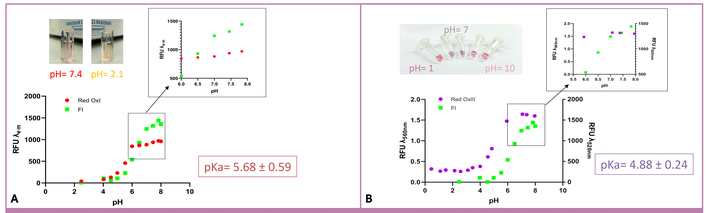

Figure 4: Stability of the fluoprophores with pH. A) Fluorescence dependence on pH of Red-OxI (12.5μM) and FI (5μM) over the pH range of 2-8, at 25°C. **B)** Fluorescence dependence on pH of Red-OxIII (9.5μM) and FI (5μM) over the pH range of 0.5-8, at 25°C.

Characterization of Red-BI

Spectroscopic properties	
λ_{max} (nm)	385
ε ($M^{-1}.cm^{-1}$)	1573

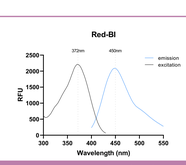

Figure 5: Spectroscopic characterization of Red-BI. Excitation and emission spectrum of Red-BI (100 μM) in sodium phosphate buffer 10mM pH= 7.4.

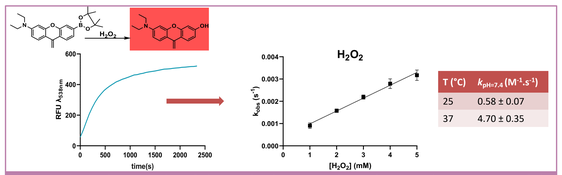

T (°C)	$k_{pH=7.4}$ ($M^{-1}.s^{-1}$)
25	0.58 ± 0.07
37	4.70 ± 0.35

Figure 6: Kinetic characterization of the reaction between Red-BI and H_2O_2. Right: Time course of the fluorescence emission change upon oxidation of Red-B (50μM) by H_2O_2 (3mM). Left: Effect of H_2O_2 concentrations on the observed rate constant (k_{obs}), determined at 25°C and 37°C, pH 7.4.

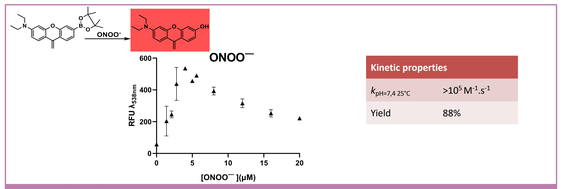

Kinetic properties	
$k_{pH=7.4\ 25°C}$	$>10^5\ M^{-1}.s^{-1}$
Yield	88%

Figure 7: Effect of peroxynitrite concentration in fluorescence of Red-BI. Fluorescence dependence of Red-B(50μM) as a function of peroxynitrite concentration at 25°C, pH 7.4.

Conclusions

- Red-BI was obtained through a five-step synthetic route with moderate overall yield.
- Red-OxI was characterized and showed optimal spectroscopic properties (λ_{exc}= 511nm; λ_{em}= 538nm ; τ_F= (τ_{F1}=0.29ns (44.25%), τ_{F2} =4.19ns (38. 13%), τ_{F3} = 1.3ns (17.63%)); Φ_F= 0.092; ε= 67000 $M^{-1}.cm^{-1}$).
- Red-OxIII was also characterized, exhibiting a longer emission wavelength but lower quantum yield and molar absorptivity than Red-OxI. (λ_{exc}= 530nm; λ_{em}= 565nm , Φ_F= 0.045, ε_M= 7133 $M^{-1}.cm^{-1}$).
- The pKa values were determined as 5.68 ± 0.59 and 4.88 ± 0.24 for Red-OxI and Red-OxIII, respectively, showing good stability at physiological pH.
- Both fluorophores showed no significant oxygen-dependent quenching effect on fluorescence within the concentration range studied.
- The reaction between Red-BI and H_2O_2 followed second-order kinetics, with rate constants at pH 7.4 of $k_{25°C}$=(0.58 ± 0.07), $k_{37°C}$=(4.70 ± 0.35).
- Red-BI showed dose-dependent reactivity with $ONOO^-$, with a yield of 88% and an estimated rate constant $>10^5\ M^{-1}.s^{-1}$.
- Further studies will allow us to validate the probe as a tool for enabling accurate cellular detection of peroxynitrite offering new insights into the role of oxygen in oxidant production within the cellular microenvironment.